Building Brownian bridges with Fermi–Dirac statistics to connect polymer loops and single file diffusion.

Wenwen Huang,[1] Yen Ting Lin,[1] Daniela Frömberg,[1] Jaeoh Shin,[1] Frank Jülicher,[1] and Vasily Zaburdaev[1]

[1] *Max Planck Institute for the Physics of Complex Systems, Nöthnitzer Str. 38, D-01187 Dresden, Germany*

Very often complex biological phenomena lead to a gold pot of statistical physics problems. In this article, we show how by reformulating the problem of chromosomal loop oscillations in the language of Brownian bridges we can unfold it into a set of related models from different fields of statistical physics and analytically solve them by essentially the same approach. We first demonstrate that a pinned polymer loop in an external force field can be approximated by a combination of Brownian bridge and Fermi-Dirac statistics, while the exact solution can be obtained via the Fermion integer partition problem. Next analogy we explore is to the asymmetric simple exclusion process with reflecting boundaries. With the help of the generalized Bethe-ansatz we are able to analytically solve for its time evolution and thus gain access to the relaxation times. Finally, in a way of demonstrating the results of such unexpected interplay of analogies, we show that thus calculated relaxation times can be used to quantify non-equilibrium dynamics of polymer loops in a biological setting. Thus we provide a unifying theoretical approach to a set of prototypical models of statistical physics which are of a broad interest to the fields of polymer physics, number theory, exclusion processes and single-file diffusion.

I. INTRODUCTION

Through the decades of DNA research it has been demonstrated that simple polymer models are extremely powerful tools to quantify various biological phenomena involving dynamics and statistics of DNA molecules: from *in vivo* mechanical properties of stretched DNA strands [] to *in vitro* chromosomal territories [], and hiC data []. Simple models, like the freely jointed chain or random coil model [], often combine analytical tractability and predictive power. Recently we have considered a problem of chromosome alignment by the drag forces during meiosis in fission yeast []. In polymer language this problem can be reformulated as finding the statistics of a pinned polymer loop in a uniform external force field. By mapping the original biological question to essentially a random walk problem we could solve for statistics of chromosomes in quite complex three-dimensional geometry with constraints. However, the developed theory only delivered predictions for the equilibrium setting, while leaving the dynamics of the process beyond its reach.

In this paper, we show how the one-dimensional version of the pinned polymer loop problem serves as a starting point of a chain of unexpected analogies that interlink several fields of statistical physics. A synergy of the Brownian bridge theory and Fermi-Dirac statistics serves as an asymptotic approximation of the polymer loop statistics. However, exact solution can also be found by solving the fermion number partition problem. We next notice that the dynamics of the pinned polymer loop in an external force field can be mapped to an asymmetric simple exclusion process (ASEP) with reflecting boundary conditions. Via this link we can, on the one hand, immediately solve for the equilibrium statistics of the ASEP model and, on the other hand, investigate the dynamics of the polymer loop by means of the ASEP approach. Remarkably, the dynamics of the ASEP model can be solved exactly via the generalized Bethe-ansatz. We find analytical predictions for the relaxation times of the system and use them to quantify the relaxation dynamics of the three-dimensional polymer loops in different regimes. We test all analytical results with kinetic Monte-Carlo and 3D Browninan Dynamics simulations.

Our results only cover the simplest geometries, but as highlighted by the chromosome alignment problem [], they can be naturally generalized to include further additional constraints. The interrelation of various prototypical statistical physics models, which we describe here, also implies that methods developed for a particular problem can most probably be ported to the other "relative" models as well. We thus think that the theoretical results presented here will be of interest to a broad and interdisciplinary scientific community working in the fields of polymer physics, number theory, and non-equilibrium statistical physics in general.

The next Section II of the manuscript is devoted to the polymer loop model and its equilibrium solution by a Brownian bridge theory and relation to the integer number partition theory. We then turn to the dynamics and the ASEP framework in Sec.III. In Sec.IV, we illustrate how the ASEP model can be utilized to study the polymer relaxation dynamics. The last Section is reserved for the discussion and conclusions.

II. STATISTICS OF THE ONE-DIMENSIONAL PINNED POLYMER LOOP

A polymer loop is a ubiquitous subject in polymer research pertinent to many important biological phenomena []. For example, fission yeast uses the viscous drag force to suppress fluctuations and align chromosomes for recombination by pulling on chromosomes shaped in a

loop []. For a constant pulling speed this setting is equivalent to a pinned polymer loop in the uniform external force field []. We start by setting up a one dimensional model of this process. See Fig. 1 for a sketch of the model.

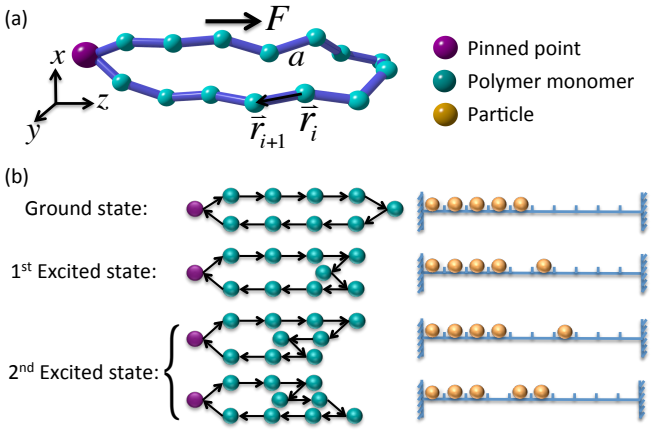

FIG. 1. Schematic figure for the model.

We consider a classical freely jointed chain model consisting of L beads connected by L rods; the rod length corresponds to the Kuhn length a of the polymer. The position of the i^{th} bead is denoted by x_i, $i \in \{0, 1, \ldots, L\}$. The looping condition suggests $x_0 = x_L = 0$. A constant external force F acts on every bead (except of pinned ones) and points in the positive direction of the x-axis. We define the orientation of the i^{th} rod as $e_j := (x_{j+1} - x_j)/a$ and therefore $x_i = a\sum_{j=0}^{i} e_j$ where $e_j = \pm 1$ and $i, j \in \{0, 1, \ldots, L-1\}$. In addition to regular forces, there are random stochastic forces acting on the chain. We will quantify their effect by an effective temperature T. We do not consider the volume exclusion effects and bending energy in this model.

Note that in the absence of force this model is equivalent to a trajectory of a one-dimensional unbiased random walk consisting of L steps, where each step corresponds to a monomer (rod) in the chain. This random walk, however, has to start and end at the same point to fulfil the loop constraint. In mathematics, it is known as the Brownian bridge problem and can be solved to find the statistics of every bead position to be Gaussian with its variance depending on the number of the bead []. Therefore we can outline the strategy of solving the problem with a non-zero force: first find how the statistics of random walk steps changes in the presence of force and then enforce the Brownian bridge condition to form a loop.

To find the statistics of random walk steps (rod orientations) we write down the potential energy of the system:

$$E = -\sum_{i=0}^{L-1} F x_i = -Fa \sum_{i=0}^{L-1}\sum_{j=0}^{i} e_j, \tag{1}$$

We now map the polymer model to a particle system. Note that the state of rod orientation is binary, $e_j \in \{-1, +1\}$. We can map it to the state of a lattice site which is either occupied by a particle, $Z_j = 1$, when the rod points along the force or empty, $Z_j = 0$, if the rod points against the force. The relation between Z_j and e_j is defined by a simple variable transformation $Z_j := (e_j + 1)/2$. The actual positions of polymer beads are obtained by the back transformation

$$x_i = a\sum_{j=0}^{i} e_j = a\left(2\sum_{j=0}^{i} Z_j - i\right). \tag{2}$$

By exchanging the order of the double summation in Eq. (1) and utilizing the loop condition $\sum_{j=0}^{L-1} e_j = 0$ we arrive at

$$E = \tilde{E} + \Delta E \sum_{j=0}^{L-1} j Z_j, \tag{3}$$

where $\tilde{E} = -L(L-1)\Delta E/2$ and $\Delta E = 2Fa$. The loop condition implies a hard constraint of the total number of the particles $\sum_{j=0}^{L-1} Z_j = L/2$ (there has to be equal number of steps along and against the force field to return to the origin).

A. Fermi-Dirac statistics of rod orientations

In the energy expression (3) one can immediately recognize the energy of a system of $L/2$ Fermions distributed over L equidistant energy levels $0, \Delta E, \ldots, (L-1)\Delta E$, where Z_j can be interpreted as an occupation number. Clearly the lowest energy of the system corresponds to $Z_j = 1$ for $j < L/2$ and $Z_j = 0$ otherwise (fully stretched polymer loop). However, when the system is in contact with the thermal bath at temperature $T > 0$, it is possible to find other configurations. The equilibrium Gibbs measure defines the probability of the system to be in a certain configuration via the corresponding exponential Boltzmann factor. Interestingly, there are two possibilities to calculate those probabilities.

The fixed total number or particles ($L/2$) corresponds to a picture of the *canonical ensemble* [**?** **?**]: the system does not exchange particles with its environment. However, the technical difficulty here is in finding all degenerate microscopic states corresponding to the given total energy of the system. Before venturing in this calculation we first look at the alternative, approximate solution.

An alternative approach is to relax the fixed-number constraint, and use the *grand canonical ensemble*, which allows exchange of particles with an external reservoir [**?** **?**], derive the probability distribution of the microscopic states to construct a random walk model, and then finally use the Brownian bridge condition to re-enforce the fixed-number constraint [**?**]. Under these assumptions, the statistics of the particles is now given by a

solution to the standard fermionic problem. The probability distribution of Z_j is the *Fermi–Dirac* distribution: [? ?]

$$\mathbb{P}\{Z_j = 1\} = \left\{1 + \exp\left[\frac{\Delta E\,(j-\mu)}{k_B T}\right]\right\}^{-1}, \tag{4a}$$

$$\mathbb{P}\{Z_j = 0\} = 1 - \mathbb{P}\{Z_j = 1\}, \tag{4b}$$

with a chemical potential $\mu = (L-1)/2$ obtained from the requirement that on average there are $L/2$ particles in the system. Noting the relation of Z_j and the orientation of j^{th} rod $e_j = (2Z_j - 1)$, the probabilities (4a) can be used to compute the distribution of e_j. The Fermi–Dirac distribution shows that in the presence of the external force field the first half of the steps is biased in the direction of force, whereas the second half of steps has higher probability of pointing against the force field. We emphasize that only in the picture of the grand canonical ensemble, the probability distributions of each rod orientation are mutually independent.

Knowing the probability distribution of the occupation number (rod orientation), their mean and variance can be easily calculated:

$$\mathbb{E}[Z_j] = \mathbb{P}\{Z_j = 1\}, \tag{5a}$$

$$\mathrm{var}[Z_j] = \mathbb{P}\{Z_j = 1\}\cdot(1 - \mathbb{P}\{Z_j = 1\}) - \mathbb{E}[Z_j]^2. \tag{5b}$$

Now that we know the statistics of individual steps we can construct the corresponding random walk process. Let us look at its trajectory connecting beads k and l, $l > k$ and the corresponding propagator $\rho(x_l = x|x_k = 0)$. Remarkably, according to the Lindeberg-Feller central limit theorem [] this propagator is Gaussian with the mean and variance equal to the sum of mean and variance of all individual steps leading from bead k to l. We therefore found the statistics of random walks governing the polymer loop in the presence of the external force field. However, due to the grand canonical approach, such random walks would return to the origin only on average. This random walk properly reproduces the mean position of every bead, but it it is not enough to estimate the fluctuations of its position. To work out the variance of the bead position we have to enforce the loop condition.

B. Imposing the Brownian bridge condition

The Brownian bridge condition is a straightforward formulation of the condition that a bead with an index i is a part of the loop of length L. The bead i belongs to the loop if two pieces of random walk trajectory of length i and $L-i$ respectively can meet at the position of the bead and belong to the same loop. Thus the probability density function of finding the bead in a given coordinate x is given by

$$\rho^L(x_i = x) = \frac{\rho(x_i = x|x_0 = 0)\,\rho(x_{L-i} = x|x_L = 0)}{\rho(x_L = 0|x_0 = 0)}, \tag{6}$$

where $\rho(x_k = x|x_j = 0)$ are the propagators of the corresponding random walk process. In case of the pinned polymer loop those propagators are Gaussian distributions with a mean and variance obtained as a sum of means and variances of all contributing individual steps of the random walk. Importantly, because each propagator entering the above Eq.(6) is Gaussian, the resulting $\rho^L(x_i = x)$ is Gaussian as well. Its variance is given by

$$\mathrm{var}\left[x_i^L\right] = \frac{\sum_{j=0}^{i}\mathrm{var}[Z_j]\sum_{j=L-i}^{L}\mathrm{var}[Z_j]}{\sum_{j=0}^{L}\mathrm{var}[Z_j]} \tag{7}$$

We can now use these results and compare with direct Monte-Carlo simulations of the one-dimensional pinned polymer loop in the external force field. In Fig. 2 we plot the mean (a) and variance (b) of every bead position for different strengths of the external force field. With increasing force the polymer becomes more stretched and fluctuations decrease. In the limit of zero force we recover the well known result of the standard Brownian bridge problem. Although calculating the sums involved in the estimation of the mean and variance does not present any particular difficulty, for not too small temperatures the sums can be approximated by integrals and evaluated explicitly (see Appendix A for details).

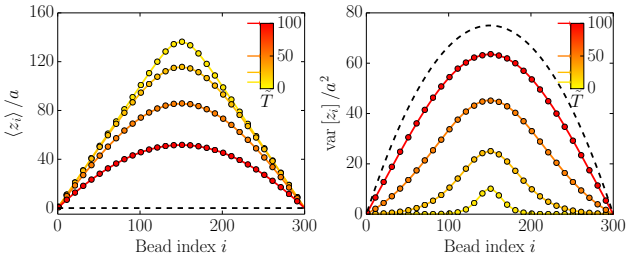

FIG. 2. Mean and variance of the 1D polymer loop.

Therefore in this section we have shown that the combination of the Fermi–Dirac statistics following from the grand canonical treatment of the system together with the Brownian bridge condition for random walks allowed us to find an excellent approximation for the statistics of the pinned polymer loop. In the next section, for the sake of completeness we show how the same problem can be addressed exactly in the canonical ensemble picture.

C. Fermion integer number partition theory

Although the above approach accurately estimates the mean and variance of equilibrium position of j bead, it is an approximated theory. Exact analytic solution is possible in this particular model and helps to establishe links to the number theory and theory of ASEP. First we change the basis of the fermionic system from its microscopic configurations $\{Z_0, Z_1, \ldots, Z_{L-1}\}$ to the total energy of the system. Clearly, the energy can only take

values $E_0, E_0 + \Delta E, \ldots, E_0 + L^2\Delta E/4$ where E_0 is the ground state. In this picture, the probability space is a one-dimensional lattice with finite support. Without loss of generality, we set the constant energy $E_0 = 0$ and $\Delta E = 1$. The difficulty of this basis is to determine the degeneracy of the microscopic states which have the same energy $E \in \{0, 1, \ldots L^2/4\}$, sometimes referred to as the "density of the state" in statistical mechanics [**?**] and condensed matter physics [**?**]. We denote the number of microscopic states with energy E to be $g(E)$; once $g(E)$ is known, the partition function of the system can be formally derived in the canonical ensemble picture

$$\mathcal{Z}(T) = \sum_{E=0}^{L^2/4} g(E) \exp\left(-\frac{E}{k_B T}\right), \tag{8}$$

and consequently the equilibrium properties of the system can be derived from it.

Interestingly the problem of finding $g(E)$ can be solved with the help of the closely related problem of integer partition in number theory [**?**]. The connection can be seen in the following way. We label the micro-state of the system by how many energy units E_i a fermion with an index i is excited from its ground state. The total energy of the system is

$$E = \sum_{i=1}^{L/2} E_i, \tag{9a}$$

and by construction we have a constraint

$$L/2 \geq E_1 \geq E_2 \geq \ldots \geq E_{L/2} \geq 0. \tag{9b}$$

Equations (9) constitutes a restricted partition of the integer E: $g(E)$ describes possible ways to partition an integer E into $L/2$ non-increasing parts [**?**].

A very intuitive way to visualize the microscopic configurations is to use the Young diagram [**?**], shown in the right panel of Fig. 1. The black box in the row i denotes the excited energy E_i. With the constraint (9b), each row can have at most $L/2$ black boxes, and the number of black boxes in $(i+1)^{\text{th}}$ row cannot exceed the that in i^{th} row. Then, $g(E)$ is the number of possibilities to arrange E black boxes onto the $L/2 \times L/2$ "checkerboard". From the number theory [**?**] the number of ways to put E black boxes onto an $K \times L$ checkerboard with non-increasing number of black boxes per row, $\pi(K, L, E)$, can be calculated. In our case $g(E) = \pi(L/2, L/2, E)$. Moreover we can find its generating function:

$$\Phi(q) := \sum_{E=0}^{L^2/4} g(E) q^E \tag{10}$$

which turns out to be the Gaussian binomial coefficient

$$\Phi(q) = \begin{pmatrix} L \\ L/2 \end{pmatrix}_q = \frac{\prod_{j=1}^{L}\left(1-q^j\right)}{\left[\prod_{j=1}^{L/2}\left(1-q^j\right)\right]^2}. \tag{11}$$

By knowing the exact partition function we can calculate the mean and variance of each bead position. For larger L the exact result is almost indistinguishable from our approximate theory based on Brownian bridges approach. However, for sufficiently small L the difference becomes more apparent (see Fig. X in Appendix B). Thus we have demonstrated that the polymer loop model can be related and solved exactly in terms of the integer number partitioning problem. This, however, is not the last analogy we are going to utilize in this paper.

Here we have to note the connection of the considered problem to the ASEP setup on an interval with reflecting boundaries [], where an analogous partition function was calculated []. This demonstrates the equivalence of our model of pinned polymer loop to the ASEP system with reflecting boundaries with exactly one half of the lattice sites occupied by the particles. In the next sections we further exploit this analogy to study the dynamics of the polymer loop model.

III. MAPPING TO ASEP

Above we considered a one-dimensional lattice with L lattice sites filled by $L/2$ particles. So far we were concerned only with the equilibrium properties of the system. However, by noticing the analogy to the ASEP model we can step beyond equilibrium considerations and study the dynamics of our system. To establish the link of the polymer loop model and the ASEP system we need to understand the relation between polymer dynamics and hopping rules of the ASEP. A particle occupying a lattice cite corresponds to a monomer of the polymer loop pointing along the direction of force. Hopping of a particle on a lattice corresponds to the flipping of two monomers connecting to the same bead and having the opposite orientations with respect to the force field (see illustration in Fig. 3). During this flip, the bead has to travel a distance of $\pm 2a$. Indeed, just like in the exclusion process, the flip can occur only if there is a "free" lattice site. The asymmetry of the flipping results from the force acting on the beads: if as a result of the flip the bead will move along the force, it will be energetically more favourable move than flipping the bead against the force. We can now formalize such dynamics by using the language of the ASEP model [**? ?**].

We denote the rate of particle hopping to right and left with α and β respectively. From the detailed balance relation we have

$$\alpha P_n = \beta P_{n+1} \tag{12}$$

where P_n is the probability of a particle sitting on the n^{th} site. The ratio of rates (and thus of the neighboring occupation probabilities) is proportional to the Boltzmann factor with the energy difference between the two states:

$$\beta/\alpha = P_n/P_{n+1} = \exp\left(-\Delta E/k_B T\right), \tag{13}$$

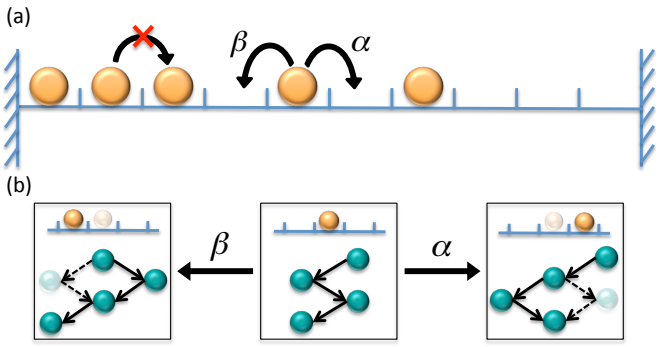

FIG. 3. Illustration of dynamics maps to ASEP.

where $\Delta E = 2Fa$. The total hopping rate of a particle is determined by the temperature:

$$\alpha + \beta = r_{\text{total}} \tag{14}$$

where r_{total} is a quantity determined by the system's temperature. Hopping of a particle to the neighboring lattice site corresponds to flipping of two monomers and the displacement of the bead by a distance of $2a$. In the force-free case this flipping happens due to random forces acting on the bead. Note that in the strictly one-dimensional setting, the monomers can not continuously turn, there are just initial and final states along or against the field. However, to quantify the time required for making a flip we can relax this limitation and imagine the bead continuously diffusing in space before it manages to travel a distance of $2a$. The diffusion constant of the bead is given by Einstein relation $D = k_B T/\gamma$, where γ is the Stokes friction $\gamma = 6\pi R\eta$, η is viscosity of the surrounding fluid, and R is the radius of the bead. We can now use this relation to estimate the time constant and therefore the total hopping rate:

$$D = \frac{4a^2}{2\tau_0} = \frac{k_B T}{\gamma}; \quad \tau_0 = \frac{2\gamma a^2}{k_B T} = r_{\text{total}}^{-1}. \tag{15}$$

Finally we obtain for the left and right hopping rates:

$$\alpha = \frac{r_{\text{total}}}{1 + \exp\left(-2Fa/k_B T\right)} \tag{16a}$$

$$\beta = \frac{r_{\text{total}} \exp\left(-2Fa/k_B T\right)}{1 + \exp\left(-2Fa/k_B T\right)} \tag{16b}$$

Hopping rates determine the dynamics of the polymer (particle) configurations, but we also need to specify the boundary conditions and if there any additional constraints on the number of particles. The pinned polymer loop corresponds to exactly $L/2$ particles hopping on L lattice sites and therefore to reflecting boundary conditions. The mapping can be generalized to other cases, for example an un-pinned polymer loop corresponds to $L/2$ particles on L lattice sites with periodic boundaries, free polymer chain corresponds to an open lattice of length L filled by arbitrary (but not larger than L) number of particles.

ASEP is one of the fundamental models of non-equilibrium statistical physics with a wealth of important analytical results. However, not so many works are dealing with the particular case of reflective boundary conditions. One important contribution is due to Schuetz [] where the partition function identical (Check!) to Eq.(**??**) was derived. Here our main motivation is to get an insight on the dynamics of the polymer loop.

IV. EXACT SOLUTION OF ASEP DYNAMICS

To illustrate the procedure of solving the dynamics, we firstly present here the simple example of two particles system. The generalization to N particles case is straight forward and details will be discussed in the Appendix.

Firstly, we write down the master equation of the particles assuming both of the particles are neither sitting on the boundary sites nor sitting on the neighboring sites:

$$\begin{aligned}\frac{dP(x_1,x_2;t)}{dt} =& \alpha P(x_1-1,x_2;t) + \beta P(x_1+1,x_2;t) \\ &+ \alpha P(x_1,x_2-1;t) + \beta P(x_1,x_2+1;t) \\ &- 2(\alpha+\beta)P(x_1,x_2;t)\end{aligned} \tag{17}$$

where $P(x_1,x_2;t)$ is the probability of configuration (x_1,x_2) at time t. Let us now consider the special cases separately. One can write down the special master equation when either particle is sitting on the boundary sites. The reflecting boundary condition can be derived by assuming Eq. (17) is valid in the whole space and then do a subtraction with the master equation at the boundaries, which write as following:

$$\alpha P(0,x_2;t) = \beta P(1,x_2;t) \tag{18a}$$

$$\alpha P(x_1,L;t) = \beta P(x_1,L+1;t) \tag{18b}$$

On the other hand, the particle can not pass each other because the exclusive definition. Similarly, one can write down the special master equation when two particles are sitting at the neighboring sites and derive the constraint of exclusion as another boundary condition written as

$$\alpha\Psi(x,x) + \beta\Psi(x+1,x+1) = (\alpha+\beta)\Psi(x,x+1) \tag{19}$$

Notice that here x is a shorthand denotes $x_1 = x_2 = x$ for the collision boundaries and Eq. (19) must be valid over all the space.

Eq. (17) together with boundary conditions Eq. (18) and Eq. (19) define the dynamics of the two particles system. To solve the dynamics, let us first take the eigenmode expansion $P(x_1,x_2;t) = \sum_k \Psi_k(x_1,x_2)e^{\Lambda_k t}$. And now our task is to find Ψ_k and corresponding eigenvalue Λ_k. The main idea of generalized Bethe-ansatz is to use the general form of single particle eigenfunctions as

building blocks to construct Ψ_k. So this method generalise the standard Bethe-ansatz used in the ASEP model with periodic boundaries where the plane wave is used as building blocks. The ansatz used for searching solution here can be written as following:

$$\Psi(x_1, x_2) = \psi_1(x_1)\psi_2(x_2) + \tilde{\psi}_2(x_1)\tilde{\psi}_1(x_2) \tag{20}$$

where ψ is a function drawn from the following general form of single particle eigenfunctions:

$$\psi_s(x) = A\left(\tfrac{\alpha}{\beta}\right)^x \tag{21a}$$

$$\psi(x) = \left(\tfrac{\alpha}{\beta}\right)^{\frac{x}{2}}\left(A_+ e^{ipx} + A_- e^{-ipx}\right) \tag{21b}$$

Here, A, A_+, A_- are amplitude coefficients that will be fixed by the boundary conditions and/or normalization, p is the wave vector of excited eigenmodes, in case of single particle, $p = \frac{k\pi}{L}$.

So in Eq (20), $\psi_n(x)$ can be either stationary Eq. (21a) or non-stationary Eq.(21b). We classify ψ_1, $\tilde{\psi}_1$ as one class and ψ_2, $\tilde{\psi}_2$ as the other class. Basically, the number of classes equals to the number of particles. For one class, if it is in non-stationary modes, $\psi_n(x)$ share the same wave vector p_n with $\tilde{\psi}_n(x)$ but different amplitude coefficients $A_{n\pm}$. And if the class is in the stationary mode, then functions in the class are differentiated by amplitude coefficient A. It is important that ψ_n and $\tilde{\psi}_n$ have different amplitude coefficients. The main idea is to tune these amplitude coefficients so that $\Psi(x_1, x_2)$ satisfies the reflecting boundaries Eq. (18) and exclusive condition Eq. (19).

There are three types of $\Psi(x_1, x_2)$ depends on whether the two classes of $\psi(x)$ are stationary or non-stationary, i.e., both are stationary, both are non-stationary and one stationary one non-stationary. The first case leads to the stationary mode of the two particles system with eigenvalue $\Lambda_0 = 0$ and $\Psi_0(x_1, x_2) = A\left(\frac{\alpha}{\beta}\right)^{x_1+x_2}$. A is a constant can be fixed by normalization. However, this is not a trivial work because of the constraint $x_1 < x_2$ and related to the exact equilibrium solution. The details will be discussed in Appendix for general N particles.

The second type of $\Psi(x_1, x_2)$ can be obtained by solving the following Bethe Equation:

$$e^{i2p_1L} = \frac{a(p_1, p_2)}{a(p_2, p_1)}\frac{a(p_2, -p_1)}{a(-p_1, p_2)} \tag{22a}$$

$$e^{i2p_2L} = \frac{a(p_2, p_1)}{a(p_1, p_2)}\frac{a(p_1, -p_2)}{a(-p_2, p_1)} \tag{22b}$$

where $a(p, p') = \sqrt{\alpha\beta}e^{i(p+p')} - (\alpha+\beta)e^{ip} + \sqrt{\alpha\beta}$. The Bethe Equations (C4) are derived by substitute the ansatz into reflecting boundaries and exclusive conditions and utilize the consistency condition. See appendix for the details. The corresponding eigenvalues can be calculated by $\Lambda = \sum_{n=1}^{2} -(\alpha+\beta) + 2\sqrt{\alpha\beta}\cos(p_n)$. Notice that by solving Eq. (C4) we can get multiple pairs of roots because it is a set of nonlinear equations. And in principle, different pair of roots can lead to different eigenvalues. So we will get more than one eigenvalues here. However, one have to filter out those roots that $p_n = k\pi$ for either $n = 1$ or $n = 2$ or both. Because these solutions belong to the either the third or the first type of $\Psi(x_1, x_2)$ where the eigenfunctions and eigenvalues are not compatible with the second type.

The third type of $\Psi(x_1, x_2)$ can be solved in a similarly way of the second type. Interestingly, the resulting Bethe Equation looks like following assuming the first class is in the stationary mode

$$e^{i2p_2L} = 1 \tag{23}$$

Solve the above equation we get $p_2 = \frac{k\pi}{L}$. And the corresponding eigenvalues are $\Lambda_k = -(\alpha+\beta) + 2\sqrt{\alpha\beta}\cos(p_2)$. See details in the appendix. Notice that the eigenvalues we obtain here are exactly the same as the eigenvalues of single particle on reflecting lattice of size L. Actually, we can show later that the set of eigenvalues of $N+1$ particles system always contain the set of eigenvalues of N particles system given that they have the same lattice sites L and $N < L/2$. For $N > L/2$, one can simply apply the particle-hole duality and obtain that the spectrum of N particles system is the same as the $L - N$ particles system.

Unlike the second type of $\Psi(x_1, x_2)$ that the Bethe Equations have to be solved numerically in general, the expression of eigenvalues and eigenfunctions can be obtained analytically for the third type which are summarized as following:

$$\Lambda_k = -(\alpha+\beta) + 2\sqrt{\alpha\beta}\cos(\frac{k\pi}{L}); k = 1, 2, \ldots, L-1 \tag{24a}$$

$$\Psi_k(x_1, x_2) = A\left[\frac{\alpha}{\beta}\left(\frac{\alpha}{\beta}\right)^{x_1}\phi_k(x_2) + \left(\frac{\alpha}{\beta}\right)^{x_2}\phi_k(x_1)\right] \tag{24b}$$

Here $\phi_k(x)$ is exactly single particle non-stationary eigenfunction and A is a constant normalization coefficient. Fortunately, numerical evidence shows that the most interesting eigenvalue, i.e., the largest non-zero eigenvalue which corresponds to the slowest relaxation mode, is contained in this analytical set. See appendix for more details.

Now let us sketch the generalization from two particls to N particles system. The details are shown in appendix. The ansatz we take is written as

$$\Psi(x_1, x_2, \cdots, x_N) = \sum_{\sigma\in\mathcal{S}_N}\prod_{n=1}^{N}\psi_n^{\sigma}(x_{\sigma(n)}) \tag{25}$$

where $\mathcal{S}_N$ is the group of permutations of N elements and ψ_n^{σ} is the n^{th} class of eigenfunction drawn from Eq. (21), either stationary or non-stationary. The subscript n means all functions in the n^{th} class share the same p_n, the superscript σ means the amplitude coefficients A_n^{σ} or $A_{n\pm}^{\sigma}$ are not the same for different permutations.

The startionary solution can be obtained by constructing Ψ use only stationary ψ_s. Finnal result can be written as

$$P^e(x_1, x_2, \cdots, x_N) = q^{-\frac{N(N+1)}{2}} \binom{L}{N}_q^{-1} \prod_{j=1}^{N} q^{x_j} \quad (26)$$

here $q := \frac{\alpha}{\beta}$. The prefactor here is identical to the partition function and is consistent with our previous calculation as well as the results from Schutz[] where a method based on quantum group is utilized.

On the other hand, if all building functions are non-stationary, we can obtain the following Bethe Equations:

$$e^{i2p_nL} = \prod_{m\neq n}^{N} \frac{a(p_n, p_m)}{a(p_m, p_n)} \frac{a(p_m, -p_n)}{a(-p_n, p_m)} \quad (27)$$

Solve the Bethe Equations for p_n and the corresponding eigenvalues are $\Lambda = \sum_{n=1}^{N} -(\alpha+\beta) + 2\sqrt{\alpha\beta}\cos(p_n)$.

Now let us consider that there are N_s stationary building classed in Ψ and $N - N_s$ non-stationary classes, where $0 < N_s < N$. One can find easily that the resulting Bethe Equations are identical to the case of $N-N_s$ particles system with all building classes are non-stationary. Moreover, the corresponding eigenvalues are $\Lambda = \sum_{n=0}^{N-N_s} -(\alpha+\beta) + 2\sqrt{\alpha\beta}\cos(p_n)$. So we can conclude that the set of eigenvalues of N particles system always contain the set of eigenvalues of $N - N_s$ system given that lattice size L is fixed and $N < L/2$. This is a generalization of the result of two particles system.

Finally, we remark that the Bethe Equations have to be solved numerically in most cases. However, there is a small set of non-stationary eigenvalues and eigenvectors we can obtain analytically, which correspond to the case with just one excitation mode. The results are summarized as following:

$$\Lambda_k = -(\alpha+\beta)+2\sqrt{\alpha\beta}\cos(\frac{k\pi}{L}); k = 1, 2, \ldots, L-1 \quad (28a)$$

$$\Psi_k(x_1, x_2, \cdots, x_N) = A\sum_{n=1}^{N} \left(\frac{\alpha}{\beta}\right)^{n-1} \phi_k(x_n) \prod_{m\neq n} \left(\frac{\alpha}{\beta}\right)^{x_m} \quad (28b)$$

Notice that the set of eigenvalue is exact the single particle spectrum, and again $\phi_k(x)$ is exactly the single particle eigenfunction. Fortunately, again the numerical evidences verify that the most interesting eigenmode, i.e. the slowest relaxation mode, is contained in this set.

With the exact solution of ASEP in hand, we now extract a physical quantity that interested us, i.e. relaxation time. It is related to the largest non-zero eigenvalue Λ_1 of the system. Here we pick the largest one from the analytical set of eigenvalues and postulate that it is the largest non-zero eigenvalue. Namely, $\Lambda_1 = -(\alpha+\beta)+2\sqrt{\alpha\beta}\cos(\frac{\pi}{L})$. This statement is difficult to prove rigorously given that the Bethe Equations have to be solved numerically in most cases. However, numerical results from both direct diagonalizing the transition matrix and Kinetic Monte-Carlo simulation of the ASEP process show that the statement is indeed true. See Fig. 4 and Fig. Sx. Accordingly, the explicit form of relaxation time of the system can be written as

$$\tau = -\frac{1}{\Lambda_1} = \frac{1}{\alpha+\beta-2\sqrt{\alpha\beta}\cos(\frac{\pi}{L})} \quad (29)$$

Notice from here that the relaxation time does not depend on the number of particles on lattice. This is verified by our numerical results.

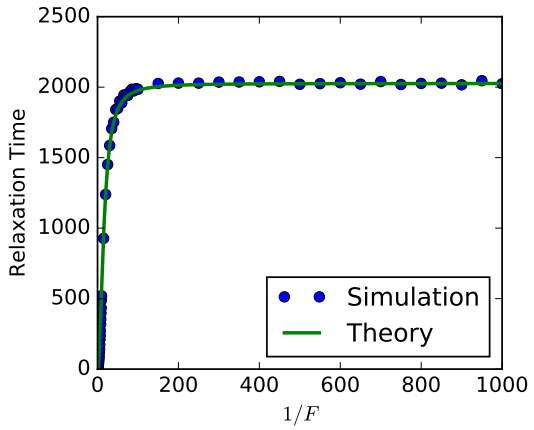

FIG. 4. relaxation time of ASEP for different force setting.

To close this subsection we would like to mention yet another connection arising from the considered solution. It is well known that ASEP models are often used as discrete counterparts of the single file diffusion process []. In single file diffusion, particles are considered to be confined to a narrow one-dimensional channel which does not allow the particles to overcome each other. As the name implies, individual particles move by normal diffusion. It can be shown that the solution for the ASEP with reflecting boundaries can be used to described the single file diffusion on a confined interval in the external force field. The crucial difference is that in case of single file diffusion particles are allowed to move continuously instead of lattice hopping in ASEP. Interestingly, the generalized Bethe-ansatz can be used to solve for the dynamics in this problem as well and we provide this solution for the sake of completeness in the Appendix B.

Starting from the biological problem of chromosome alignment we could unfold a very rich sequence of analogies and obtained the whole set of new analytical results. To make the loop complete also in current work we would like to demonstrate how these analytical results can be put to work in the applied setting.

V. RELAXATION DYNAMICS OF A POLYMER LOOP

Previously we argued that the stationary solution for the pinned polymer loop could be used to quantify the chromosome separation during meiosis in fission yeast []. However a very reasonable question is if the stationary state could be achieved in biologically relevant time scales. To answer this question we suggest to look at the relaxation dynamics of the pinned polymer loop as a function of parameters of the problem and in particular the applied external force. We performed extensive three-dimensional Brownian dynamics simulations of the relaxation process of the loop. By calculating the autocorrelation function of diameter vector defined as $\mathbf{r}_d = \mathbf{r}_{L/2} - \mathbf{r}_0$, we could extract the longest relaxation time of the polymer loop and plot it as a function of the applied force (see Fig.X). The relaxation times show the behavior very similar to our analytical prediction for the one-dimensional problem. We hypothesized that the functional form of Eq.() could be used to describe the results of the 3D simulations. Importantly, we know that the relaxation time in the limit of $F \leftarrow 0$ can be calculated from the Rouse-theory analytically in the 3D case as well. The result is identical to the 1D regime with an additional prefactor of 1/12 which arises due to the 3D noise and strictly speaking $\tau_0 \propto \frac{2\gamma a^2}{k_B T}$ rather than the equality in Eq. (15). We now can use this prefactor in the analytical formula Eq.() and plot it together with simulation results. Analytical (rescaled on the basis of the Rouse-theory) prediction matches the simulations very accurately. Note that there was no fitting involved when comparing theory and numerical data. Certainly the achieved match is a somewhat semi-empirical result, we did not provide any three-dimensional theory except for the limit $F \leftarrow 0$. Nevertheless the one-dimensional model allows us to understand exactly the mechanisms responsible for the relaxation process in the system. It also makes it plausible to suggest that our results can be rigorously extended to higher dimensions.

VI. CONCLUSIONS

We demonstrated that the problem of the pinned 1D polymer loop in the external force field can be mapped to a system of particles hopping on lattice sites (ASEP). While the polymer problem can be asymptotically solved via the Brownian bridge formalism, in the ASEP formulation it has an exact solution. ASEP advances our understanding of the system to the dynamics regime. The key technique for the ASEP model solution is the generalized Bethe-ansatz, adding up to the Fermi-Dirac statistic as yet another unexpected appearance of quantum-mechanics tools in an originally biophysical problem. Finally we could use those results to explain the force dependence of the relaxation times observed in 3D Brownian dynamics simulations.

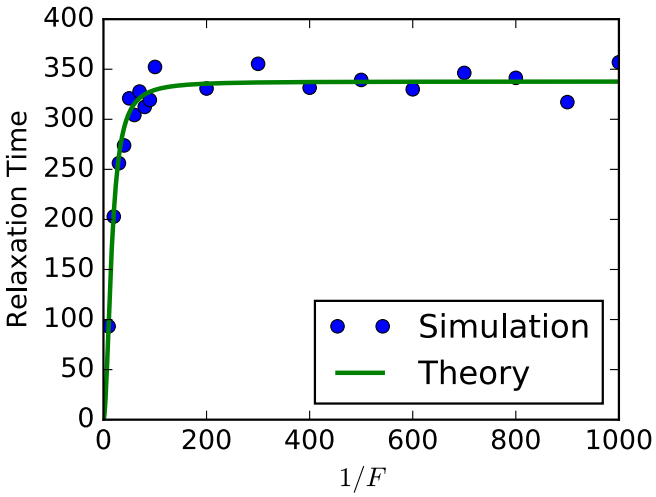

FIG. 5. relaxation time of 3D pinned polymer.

The mapping from polymer to particles is not restricted to the case of pinned polymer loop. Other situations can be investigated with the same mapping, which leads to ASEP model with different boundaries and particle numbers. Moreover, the polymer dynamics beyond 1D is also possible to model by multi-species ASEP model []. We believe that by showing the unity of such apparently different systems we pave the way to their better understanding and hopefully to further new results.

ACKNOWLEDGMENTS

We would like to acknowledge stimulating discussions with M. Majumdar and E. Frey.

Appendix A: Simulation Methods

Extensive simulations are performed in this work in order to compare with the theory, including the Monte-Carlo simulation of the ASEP system and Brownian Dynamics simulation of the 3D pinned polymer loop. For the ASEP system, Gillespie algorithm [] is employed for the simulations and we will not go into the details. Interested readers can see the references therein. On the other hand, the Brownian Dynamics simulation is more tricky and we will discuss in the following text.

As we use the simple freely jointed bead-rod model, the Brownian dynamics of the beads ignoring inertial can be written as

$$-\xi \frac{d\mathbf{r}_i}{dt} = \mathbf{F}_i^c + \mathbf{F}_i^e + \mathbf{F}_i^b + \mathbf{F}_i^{pseudo} \qquad \text{(A1)}$$

where ξ is the friction coefficient, $\mathbf{F}_i^c$ is the constraint force that keeps the rod with constant length, $\mathbf{F}_i^e$ is the

external force, $\mathbf{F}_i^b$ is the Brownian force that satisfying $\langle \mathbf{F}_i^b \rangle = \mathbf{0}$ and $\langle f_{im}^b(t) f_{jn}^b(t') \rangle = 2\xi k_B T \delta_{ij}\delta_{mn}\delta(t-t')$, and $\mathbf{F}_i^{pseudo}$ is pseudo force added in order to get correct statistics, where $\mathbf{F}_i^{pseudo} = -\frac{\partial U_{met}}{\partial \mathbf{r}_i}; U_{met} = \frac{1}{2}k_B T \ln(\det G)$, G is the metric tensor[].

The constraint force $\mathbf{F}_i^c$ is solved implicitly use the predictor-corrector algorithm by solving the constraint equations that $|\mathbf{r}_{i+1} - \mathbf{r}_i| = a$. On the other hand, in order to pin the polymer loop, we add a "phantom" rod of length zero at the pinned bead, and bond it to the origin.

In practice, we use the dimensionless term of the dynamical equations that can be obtained by the rescaling $\mathbf{r}' \to \mathbf{r}/a$; $t' \to t/(\xi a^2/k_B T)$; $\mathbf{F}' \to \mathbf{F}/(k_B T/a)$.

Appendix B: Stationary Solution of N Particles ASEP

The N particles stationary solution can be constructed as

$$P^e(x_1, x_2, \cdots, x_N) = \Psi(x_1, x_2, \cdots, x_N) = A \prod_{j=1}^{N} \left(\frac{\alpha}{\beta}\right)^{x_j} \tag{B1}$$

One can plug in the master equation check that the corresponding eigenvalue $\Lambda_0 = 0$, and also verify the exclusive condition as well as the reflecting boundaries are both fulfilled.

We now try to fix the important normalization parameter A, which corresponds to the partition function. We can rewrite A as following

$$A^{-1} = \sum_{\Omega} q^{\sum_j x_j} = \sum_{x_1 < x_2 < \cdots < x_N} q^{\sum_j x_j} \tag{B2}$$

Let us do a variable change so that

$$\sum_j x_j = E_0 + E$$

$$E_0 = 1 + 2 + \cdots + N = \frac{N(N+1)}{2}$$

We can derive that E is a integer in the range of $0, 1, \cdots, N(L-N)$. So Eq. (B2) can be rewrite as

$$A^{-1} = q^{E_0} \sum_{E=0}^{N(L-N)} g(E) q^E \tag{B3}$$

where $g(E)$ is the number of partitions of positive integer E to N parts with each of size at most $L-N$. From the number partition theory, we identify

$$\sum_{E=0}^{N(L-N)} g(E) q^E = \binom{L}{N}_q = \frac{[L]_q!}{[L-N]_q![N]_q!} \tag{B4}$$

where $[N]_q = 1 + q + q^2 + \cdots + q^{N-1}$ is called a q number, and Eq. (B4) is called the q binomial coefficient[]. So we finally arrive at

$$P^e(x_1, x_2, \cdots, x_N) = q^{-\frac{N(N+1)}{2}} \binom{L}{N}_q^{-1} \prod_{j=1}^{N} q^{x_j} \tag{B5}$$

In [], G. M. Schütz use a quantum group formalism obtained the same result with a different notation. We emphasize here that our method is much more easily to understand and no prerequisite knowledge of quantum mechanics and group theory is needed.

With the equilibrium N particle distribution, we can readily calculate the equilibrium distribution of any tagged particle. Denote he distribution of the nth particle $p_n(x)$, we have

$$\begin{aligned} p_n(x) = & \sum_{0 < x_1 < \cdots < x_{n-1} \le x-1} P^e(x_1, x_2, \cdots, x_N) \\ & \times \sum_{x < x_{n+1} < \cdots < x_N \le L} P^e(x_1, x_2, \cdots, x_N) \\ = & \, q^{(N+1-n)(x-n)} \binom{x-1}{n-1}_q \binom{L-x}{N-n}_q \Big/ \binom{L}{N}_q \end{aligned} \tag{B6}$$

Finally, the equilibrium density profile can be obtain by summing up $p_n(x)$

$$\rho(x) = \sum_{n=1}^{N} p_n(x) \tag{B7}$$

The exact result is shown in Fig. 6 and compared with the density profile we get from the Fermi-Dirac statistics. We can see that the accuracy of Fermi-Dirac approximation is actually very good.

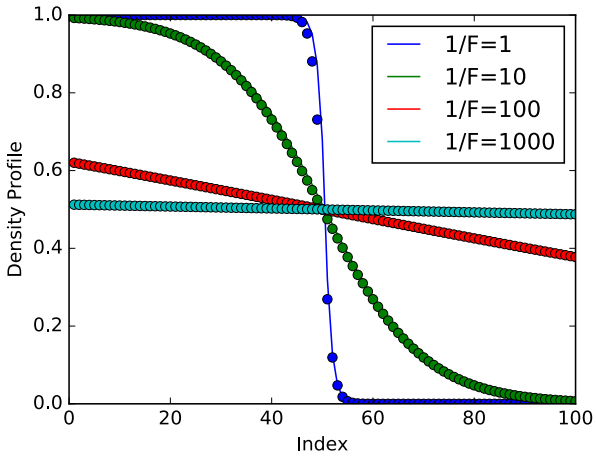

FIG. 6. density profile

Appendix C: Derivation of the Bethe Equations

To show the derivation of the Bethe Equations, we first show it in the simple two particles case and then generalise to N particles case.

Let us firstly consider the two particles non-stationary eigenmode that two classes of building functions are both non-stationary. Plug the ansatz Eq. (20) in the reflecting boundaries Eq. (18), we get

$$\frac{A_{1+}}{A_{1-}} = -\frac{\alpha - \sqrt{\alpha\beta}e^{-ip_1}}{\alpha - \sqrt{\alpha\beta}e^{ip_1}} \tag{C1a}$$

$$\frac{\tilde{A}_{1+}}{\tilde{A}_{1-}} = -\frac{\left(\alpha - \sqrt{\alpha\beta}e^{-ip_1}\right)e^{-ip_1L}}{\left(\alpha - \sqrt{\alpha\beta}e^{ip_1}\right)e^{ip_1L}} \tag{C1b}$$

$$\frac{\tilde{A}_{2+}}{\tilde{A}_{2-}} = -\frac{\alpha - \sqrt{\alpha\beta}e^{-ip_2}}{\alpha - \sqrt{\alpha\beta}e^{ip_2}} \tag{C1c}$$

$$\frac{A_{2+}}{A_{2-}} = -\frac{\left(\alpha - \sqrt{\alpha\beta}e^{-ip_2}\right)e^{-ip_2L}}{\left(\alpha - \sqrt{\alpha\beta}e^{ip_2}\right)e^{ip_2L}} \tag{C1d}$$

On the other hand, plug the ansatz into the exclusive condition Eq. (19) and use the definition of $a(p,p')$, we obtain

$$\frac{A_{1+}A_{2+}}{\tilde{A}_{1+}\tilde{A}_{2+}} = -\frac{a(p_1,p_2)}{a(p_2,p_1)} \tag{C2a}$$

$$\frac{A_{1+}A_{2-}}{\tilde{A}_{1+}\tilde{A}_{2-}} = -\frac{a(p_1,-p_2)}{a(-p_2,p_1)} \tag{C2b}$$

$$\frac{A_{1-}A_{2+}}{\tilde{A}_{1-}\tilde{A}_{2+}} = -\frac{a(-p_1,p_2)}{a(p_2,-p_1)} \tag{C2c}$$

$$\frac{A_{1-}A_{2-}}{\tilde{A}_{1-}\tilde{A}_{2-}} = -\frac{a(-p_1,-p_2)}{a(-p_2,-p_1)} \tag{C2d}$$

Notice that the ratio of amplitude coefficients calculated use different ways should be consistent, thus we have the following consistency conditions:

$$\frac{A_{1+}}{A_{1-}}\frac{\tilde{A}_{1-}}{\tilde{A}_{1+}} = \frac{A_{1+}A_{2+}}{\tilde{A}_{1+}\tilde{A}_{2+}}\frac{\tilde{A}_{2+}\tilde{A}_{1-}}{A_{2+}A_{1-}} \tag{C3a}$$

$$\frac{\tilde{A}_{2+}}{\tilde{A}_{2-}}\frac{A_{2-}}{A_{2+}} = \frac{\tilde{A}_{1+}\tilde{A}_{2+}}{A_{1+}A_{2+}}\frac{A_{1+}A_{2-}}{\tilde{A}_{1+}\tilde{A}_{2-}} \tag{C3b}$$

After substitute Eq. (C1),(C2) we arrive at the following Bethe equations:

$$e^{i2p_1L} = \frac{a(p_1,p_2)}{a(p_2,p_1)}\frac{a(p_2,-p_1)}{a(-p_1,p_2)} \tag{C4a}$$

$$e^{i2p_2L} = \frac{a(p_2,p_1)}{a(p_1,p_2)}\frac{a(p_1,-p_2)}{a(-p_2,p_1)} \tag{C4b}$$

For the case that the ansatz is constructed by one stationary and one non-stationary building function classes, the procedure is more or less the same, we can obtain the Bethe equation exact leads to the eigenvalues of single particle spectrum, i.e. $e^{i2p_2L} = 1$.

Let us not come to the N particles case, the reflecting boundaries give

$$\frac{A^{\sigma|\sigma(1)=n}_{n+}}{A^{\sigma|\sigma(1)=n}_{n-}} = -\frac{\alpha - \sqrt{\alpha\beta}e^{-ip_n}}{\alpha - \sqrt{\alpha\beta}e^{ip_n}} \tag{C5a}$$

$$\frac{A^{\sigma|\sigma(N)=n}_{n+}}{A^{\sigma|\sigma(N)=n}_{n-}} = -\frac{\left(\alpha - \sqrt{\alpha\beta}e^{-ip_n}\right)e^{-ip_nL}}{\left(\alpha - \sqrt{\alpha\beta}e^{ip_n}\right)e^{ip_nL}} \tag{C5b}$$

and the exclusive conditions implies

$$\frac{A^{\sigma}_{n\pm}A^{\sigma}_{(n+1)\pm}}{A^{\sigma|n\leftrightarrow n+1}_{n\pm}A^{\sigma|n\leftrightarrow n+1}_{(n+1)\pm}} = -\frac{a(\pm p_n,\pm p_{n+1})}{a(\pm p_{n+1},\pm p_n)} \tag{C6}$$

Finally, use the consistency conditions similar to Eq. (C3) we obtain

$$e^{i2p_nL} = \prod_{m\neq n}^{N}\frac{a(p_n,p_m)}{a(p_m,p_n)}\frac{a(p_m,-p_n)}{a(-p_n,p_m)} \tag{C7}$$

Now it would be interesting to interpret the Bethe Equation and compare with the well know Bethe Equation of periodic boundary case. We can consider Eq. (C5) as a reflector that reflects the particle and change the direction of wave vector, i.e., $p_n \leftrightarrow -p_n$. On the other hand, Eq. (C6) can be interpreted as a permutator that permutes two neighboring particles $n \leftrightarrow (n+1)$. Let us say particle 1 starts from the left side of the lattice and then permutes with all the particle at right side until reaches the right boundary (of course in case of two particles, there are only one particle at the right side), and then reflects by the boundary, become a particle traveling in the opposite direction, and then permutes with all the left side particles until reaches the left side boundary, and then reflects again, which recovers the initial state. In this sense, the particle works as if it is on a lattice with periodic boundary. Use this interpretation and the well know result of periodic Bethe Equation, once can easily recover exactly Eq. (C7).

[1] B. Alberts, A. Johnson, J. Lewis, M. Raff, K. Roberts, and P. Walter, *Molecular Biology of the Cell, Fourth Edition* (Garland Science, New York, 2002), 4th ed.

[2] J. L. Gerton and R. S. Hawley, Nat. Rev. Genet. **6**, 477 (2005).

[3] A. M. Villeneuve and K. J. Hillers, Cell **106**, 647 (2001).

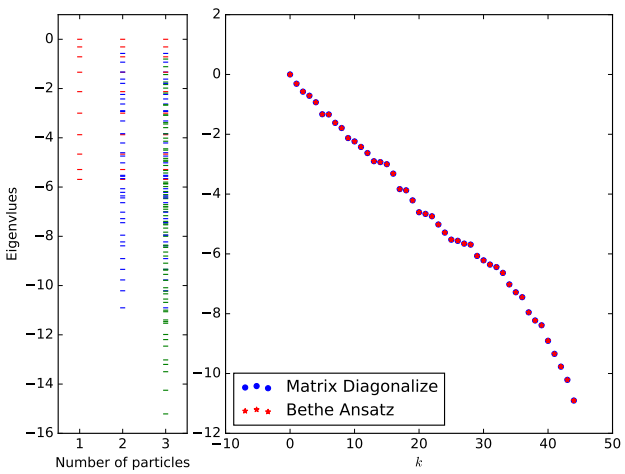

FIG. 7. eigenvalue obtained from directly diagonalizing the transition matrix and comparison with the results from Bethe-ansatz.

[4] B. D. McKee, BBA-Gene. Struct. Expr. **1677**, 165 (2004).

[5] R. Egel, *The Molecular Biology of Schizosaccharomyces pombe: Genetics, Genomics and Beyond*(Springer, Berlin-Heidelberg, 2004).

[6] L. Davis and G. R. Smith, Proc. Natl. Acad. Sci. U. S. A. **98**, 8395 (2001).

[7] P. Munz, Genetics **137**, 701 (1994).

[8] J. L. Wells, D. W. Pryce, and R. J. McFarlane, Yeast **23**, 977 (2006).

[9] See Supplemental Material at ... for detailed description of experimental procedures, numerical simulations, and the discussion of 3D fluctuations of the polymer loop.

[10] D.-Q. Ding, Y. Chikashige, T. Haraguchi, and Y. Hiraoka, J. Cell Sci. **111**, 701 (1998).

[11] S. K. Vogel, N. Pavin, N. Maghelli, F. Jülicher, and I. M. Tolić-Nørrelykke, PLoS Biol. **7**, e1000087 (2009).

[12] A. Yamamoto, C. Tsutsumi, H. Kojima, K. Oiwa, and Y. Hiraoka, Mol. Biol. Cell **12**, 3933 (2001).

[13] A. Yamamoto, R. R. West, J. R. McIntosh, and Y. Hiraoka, J. Cell Biol. **145**, 1233 (1999).

[14] V. Ananthanarayanan, M. Schattat, S. K. Vogel, A. Krull, N. Pavin, and I. M. Tolić-Nørrelykke, Cell **153**, 1526 (2013).

[15] R. Koszul and N. Kleckner, Trends Cell Biol. **19**, 716 (2009).

[16] D.-Q. Ding, A. Yamamoto, T. Haraguchi, and Y. Hiraoka, Dev. Cell **6**, 329 (2004).

[17] D. J. Wynne, O. Rog, P. M. Carlton, and A. F. Dernburg, J. Cell Biol. **196**, 47 (2012).

[18] M. Doi and S. Edwards, *The theory of polymer dynamics, International series of monographs on physics* (Clarendon Press, Oxford, 1986).

[19] Since the recombination machinery, locally altering the properties of the chromatin, becomes active only after the homologous chromosomes come to close proximity, we assume the effective temperature to be spatially uniform.

[20] D. Revuz and M. Yor, *Continuous Martingales and Brownian Motion, Grundlehren der mathematischen Wissenschaften* (Springer, Berlin-Heidelberg, 1999).

[21] L. Rogers and D. Williams, *Diffusions, Markov Processes, and Martingales: Volume 1, Foundations, Cambridge Mathematical Library* (Cambridge University Press, Cambridge, 2000).

[22] S. N. Majumdar and A. Comtet, Phys. Rev. Lett. **92**, 225501 (2004).

[23] The difference is that Brownian bridge is defined for a time continuous Brownian motion, but the equivalence to the discrete random walk problem can be demonstrated in the proper limit.

[24] In fact it is a Gaussian with a cut off on the tails of the distribution due to the fixed length of the polymer. This effect is analogous to the effect of the finite velocity of diffusing particles. It does not change the Gaussian nature of the bulk of the distribution and only affects its far tails.

[25] Interestingly, it can be shown that the statistics of rod orientations in a one-dimensional case is given by the Fermi-Dirac distribution. This problem will be discussed in detail elsewhere.

[26] W. Greene, *Econometric Analysis* (Prentice Hall, Upper Saddle River, NJ, 2008).

[27] K. Athreya and S. Lahiri, *Measure Theory and Probability Theory, Springer Texts in Statistics* (Springer, New York, 2006).

[28] D. Zickler and N. Kleckner, Annu. Rev. Genet. **33**, 603 (1999).

[29] G. A. Cromie, R. W. Hyppa, A. F. Taylor, K. Zakharyevich, N. Hunter, and G. R. Smith, Cell **127**, 1167 (2006).

[30] W. F. Marshall, J. F. Marko, D. A. Agard, and J. W. Sedat, Curr. Biol. **11**, 569 (2001).

[31] S. P. Alexander and C. L. Rieder, J. Cell Biol. **113**, 805 (1991).

[32] I. Kalinina, A. Nandi, P. Delivani, M. R. Chacón, A. H. Klemm, D. Ramunno-Johnson, A. Krull, B. Lindner, N. Pavin, and I. M. Tolić-Nørrelykke, Nat. Cell Biol. **15**, 82 (2013).

[33] K. Bystricky, P. Heun, L. Gehlen, J. Langowski, and S. M. Gasser, Proc. Natl. Acad. Sci. U. S. A. **101**, 16495 (2004).

[34] Y. Cui and C. Bustamante, Proc. Natl. Acad. Sci. U. S. A. **97**, 127 (2000).

[35] J. Langowski, Eur. Phys. J. E **19**, 241 (2006).

[36] A. Rosa and R. Everaers, PLoS Comput. Biol. **4**, e1000153 (2008).

[37] D.-Q. Ding, N. Sakurai, Y. Katou, T. Itoh, K. Shirahige, T. Haraguchi, and Y. Hiraoka, J. Cell Biol. **174**, 499 (2006).

[38] A. Gennerich, A. P. Carter, S. L. Reck-Peterson, and R. D. Vale, Cell **131**, 952 (2007).

[39] S. Toba, T. M. Watanabe, L. Yamaguchi-Okimoto, Y. Y. Toyoshima, and H. Higuchi, Proc. Natl. Acad. Sci. U. S. A. **103**, 5741 (2006).

[40] Y. Zhang and D. W. Heermann, PLoS ONE **6**, e29225 (2012).

[41] Y. Zhang, S. Isbaner, and D. W. Heermann, Front. Phys. **1**, DOI=10.3389/fphy.2013.00016 (2013).